eNeuro

Research Article: New Research

Disorders of the Nervous System

Parvalbumin Interneuron Dysfunction in a Thalamo-Prefrontal Cortical Circuit in *Disc1* Locus Impairment Mice

Kristen Delevich,[1,2] Hanna Jaaro-Peled,[4] Mario Penzo,[3] Akira Sawa,[4] and Bo Li[1,2]

https://doi.org/10.1523/ENEURO.0496-19.2020

[1]Cold Spring Harbor Laboratory, Cold Spring Harbor, NY 11724, [2]Watson School of Biological Sciences, Cold Spring Harbor Laboratory, Cold Spring Harbor, NY 11724, [3]National Institute of Mental Health, Bethesda, MD 20892, and [4]Department of Psychiatry, Johns Hopkins University School of Medicine, Baltimore, MD 21287

Abstract

Altered cortical excitation-inhibition (E-I) balance resulting from abnormal parvalbumin interneuron (PV IN) function is a proposed pathophysiological mechanism of schizophrenia and other major psychiatric disorders. Preclinical studies have indicated that *disrupted-in-schizophrenia-1* (*Disc1*) is a useful molecular lead to address the biology of prefrontal cortex (PFC)-dependent cognition and PV IN function. To date, PFC inhibitory circuit function has not been investigated in depth in *Disc1* locus impairment (LI) mouse models. Therefore, we used a *Disc1* LI mouse model to investigate E-I balance in medial PFC (mPFC) circuits. We found that inhibition onto layer 2/3 excitatory pyramidal neurons in the mPFC was significantly reduced in *Disc1* LI mice. This reduced inhibition was accompanied by decreased GABA release from local PV, but not somatostatin (SOM) INs, and by impaired feedforward inhibition (FFI) in the mediodorsal thalamus (MD) to mPFC circuit. Our mechanistic findings of abnormal PV IN function in a *Disc1* LI model provide insight into biology that may be relevant to neuropsychiatric disorders including schizophrenia.

Key words: disrupted-in-schizophrenia-1; feedforward inhibition; mediodorsal thalamus; parvalbumin interneurons; prefrontal cortex

Significance Statement

A popular theory suggests that dysregulation of fast-spiking parvalbumin interneurons (PV INs) and elevated excitation-inhibition (E-I) balance contribute to the pathophysiology of various psychiatric disorders. Previous studies suggest that genetic perturbations of the *disrupted-in-schizophrenia-1* (*Disc1*) gene affect prefrontal cortex (PFC)-dependent cognition and PV IN function, but synaptic and circuit physiology data are lacking. Here, we provide evidence that the presynaptic function of PV INs in the medial PFC (mPFC) is altered in *Disc1* LI mice and that E-I balance is elevated within a thalamofrontal circuit known to be important for cognition. These findings may contribute to our understanding of the biology that gives rise to cognitive symptoms in a range of neuropsychiatric disorders.

Introduction

Parvalbumin interneurons (PV INs) provide powerful somatic inhibition to excitatory pyramidal neurons and regulate excitation-inhibition (E-I) balance (Isaacson and Scanziani, 2011). Prefrontal PV INs are implicated in working memory (WM) function (Cardin et al., 2009; Fries, 2009; Sohal et al., 2009; Murray et al., 2015; Ferguson and Gao, 2018b) and have emerged from human postmortem studies as a key node of interest in the pathophysiology of schizophrenia (Beasley and Reynolds,

Received November 26, 2019; accepted January 27, 2020; First published February 6, 2020.
The authors declare no competing financial interests.

Author contributions: K.D. and B.L. designed research; K.D. and M.P. performed research; H.J.-P. and A.S. contributed unpublished reagents/analytic tools; K.D. analyzed data; K.D., A.S., and B.L. wrote the paper.

1997; Hashimoto et al., 2003; Lewis et al., 2012). Therefore, dysregulation of E-I balance via altered PV IN function is a potential pathophysiological mechanism of particular relevance to cognitive symptoms of neuropsychiatric diseases, including schizophrenia. Cognitive impairment is seen in first-degree relatives of individuals with a range of major mental illnesses (Cannon et al., 2000; Myles-Worsley and Park, 2002; Snitz et al., 2006), suggesting that these processes are partly heritable and may be better understood through investigation of promising genetic and molecular leads.

A translocation in the gene *disrupted-in-schizophrenia-1* (*Disc1*) was first reported in a Scottish pedigree as a rare but penetrant genetic risk factor that may account for a wide range of major mental illnesses such as depression and schizophrenia (Millar et al., 2000). This suggests that biological pathway(s) involving the multifunctional hub protein DISC1 contribute to cognitive and behavioral dimensions that are disrupted in neuropsychiatric illnesses (Niwa et al., 2016). While DISC1 is not a common genetic variant associated with schizophrenia in large population samples (Schizophrenia Working Group of the Psychiatric Genomics C, 2014), it can serve as a molecular lead to study the biology underlying important constructs/dimensions that are relevant to major mental illness (Niwa et al., 2016). Work in mouse models has revealed the importance of DISC1 in neurodevelopment (Kamiya et al., 2005; Ishizuka et al., 2007, 2011; Mao et al., 2009; Niwa et al., 2010), synaptic function (Hayashi-Takagi et al., 2010; Wang et al., 2011; Maher and LoTurco, 2012; Sauer et al., 2015; Seshadri et al., 2015; Wei et al., 2015), and cognitive processing (Brandon and Sawa, 2011). WM impairments are consistently reported across *Disc1* mouse models (Koike et al., 2006; Clapcote et al., 2007; Li et al., 2007; Kvajo et al., 2008; Lipina et al., 2010; Niwa et al., 2010; Brandon and Sawa, 2011; Lee et al., 2013). Furthermore, a variety of *Disc1* mouse models exhibit reduced prefrontal PV expression (Hikida et al., 2007; Shen et al., 2008; Ibi et al., 2010; Niwa et al., 2010; Ayhan et al., 2011; Lee et al., 2013). While these data are suggestive that PV INs may be particularly affected by *Disc1* perturbation, evidence from synaptic and circuitry physiology is lacking.

Here, we investigated the synaptic and circuit level function of PV INs within medial prefrontal cortex (mPFC) circuits of mice heterozygous for the *Disc1* locus impairment (LI) allele, in which the majority of *Disc1* isoforms are abolished (Seshadri et al., 2015; Shahani et al., 2015). We found that *Disc1* LI was associated with elevated E-I balance and altered PV IN function in mPFC circuits relevant to cognition.

This work was supported by a National Institutes of Health (NIH) training grant (K.D.), NIH Grants R01MH101214 and R01MH108924 (to B.L.) and R01MH094268 and R01MH105660 (to A.S.), a National Alliance for Research on Schizophrenia and Depression grant (B.L.), the Wodecroft Foundation (B. L.), the Stanley Family Foundation (B.L.), Simons Foundation Autism Research Initiative (B.L.), Louis Feil Trust (B.L.), and the Cold Spring Harbor Laboratory and Northwell Health Affiliation (B.L.).

Acknowledgements: We thank members of the B.L. laboratory for discussions.

Correspondence should be addressed to Kristen Delevich at delevich@berkeley.edu.

https://doi.org/10.1523/ENEURO.0496-19.2020

Materials and Methods

Animals

Mice were group housed under a 12/12 h light/dark cycle (9 A.M. to 9 P.M. light), with food and water freely available. Both male and female mice were used. All procedures involving animals were approved by the Institutional Animal Care and Use Committee of Cold Spring Harbor Laboratory and conducted in accordance with the National Institutes of Health guidelines. The *PV-Cre* (http://jaxmice.jax.org/strain/008069.html), *SOM-Cre* (http://jaxmice.jax.org/strain/013044.html), and *Ai14* (https://www.jax.org/strain/007914) mice were described previously (Hippenmeyer et al., 2005; Madisen et al., 2010; Taniguchi et al., 2011). We previously generated the *Disc1* LI mice, which harbor a deletion (6.9 kb) encompassing the first three exons of the *Disc1* gene (Seshadri et al., 2015). The majority of DISC1 isoforms are abolished in mice homozygous for the *Disc1* LI allele (Seshadri et al., 2015), and in the current study we used mice that harbored one *Disc1* LI allele (+/−). All mice were bred onto C57BL/6 background for at least five generations.

Viral vectors

Adeno-associated virus (AAV) vectors AAV-CAG-ChR2 (H134R)-YFP and AAV-eF1a-DIO-ChR2(H134R)-YFP were produced as AAV2/9 serotype by the University of North Carolina Vector Core and have been previously described (Zhang et al., 2007; Delevich et al., 2015). All viral vectors were stored in aliquots at −80°C until use.

Stereotaxic surgery

Mice aged postnatal day (P)40–56 were used for all surgeries. Unilateral viral injections were performed using previously described procedures (Li et al., 2013) at the following stereotaxic coordinates: MD: –1.58 mm from bregma, 0.44 mm lateral from midline, and 3.20 mm ventral from cortical surface; dorsal mPFC: 1.94 mm from bregma, 0.34 mm lateral from midline, and 0.70 mm ventral from cortical surface. Surgical procedures were standardized to minimize the variability of AAV injections. To ensure minimal leak into surrounding brain areas, injection pipettes remained in the brain for ~5 min after injection before being slowly withdrawn. The final volume for AAV-CAG-ChR2(H134R)-YFP injected into MD was 0.3–0.35 μl, and for AAV-eF1a-DIO-ChR2(H134R)-YFP injected into dorsal mPFC was 0.5 μl. The titer for the viruses was ~10^{12} viral particles/ml. For experiments in which mPFC inhibitory INs were optogenetically stimulated (Fig. 2) mice were injected at P56 and approximately two weeks were allowed for viral expression before recording. For experiments in which MD axons within mPFC were optogenetically stimulated (Figs. 3, 5) mice

were injected at P40–45 and approximately four weeks were allowed for viral expression before recording. For each of these experiments, littermates were injected and recorded at the same age to control for expression duration between genotypes.

Electrophysiology

Mice were anaesthetized with isoflurane and decapitated, whereupon brains were quickly removed and immersed in ice-cold dissection buffer (110.0 mM choline chloride, 25.0 mM $NaHCO_3$, 1.25 mM NaH_2PO_4, 2.5 mM KCl, 0.5 mM $CaCl_2$, 7.0 mM $MgCl_2$, 25.0 mM glucose, 11.6 mM ascorbic acid, and 3.1 mM pyruvic acid, gassed with 95% O_2 and 5% CO_2). Coronal slices (300 μm in thickness) containing mPFC were cut in dissection buffer using a HM650 Vibrating Microtome (Thermo Fisher Scientific), and were subsequently transferred to a chamber containing artificial CSF (ACSF; 118 mM NaCl, 2.5 mM KCl, 26.2 mM $NaHCO_3$, 1 mM NaH_2PO_4, 20 mM glucose, 2 mM $MgCl_2$, and 2 mM $CaCl_2$, at 34°C, pH 7.4, gassed with 95% O_2 and 5% CO_2). After ~30 min of recovery time, slices were transferred to room temperature and were constantly perfused with ACSF.

The internal solution for voltage-clamp experiments contained 140 mM potassium gluconate, 10 mM HEPES, 2 mM $MgCl_2$, 0.05 mM $CaCl_2$, 4 mM MgATP, 0.4 mM Na_3GTP, 10 mM Na_2-phosphocreatine, 10 mM BAPTA, and 6 mM QX-314 (pH 7.25, 290 mOsm). Electrophysiological data were acquired using pCLAMP 10 software (Molecular Devices). Miniature IPSCs (mIPSCs) were recorded in the presence of tetrodotoxin (1 μM), APV (100 μM), and CNQX (5 μM). Miniature EPSCs (mEPSCs) were recorded in the presence of tetrodotoxin (1 μM) and picrotoxin (100 μM). Data were analyzed using Mini Analysis Program (Synaptosoft). For the mIPSCs and mEPSCs, we analyzed the first 300 and 250 events, respectively, for each neuron. The parameters for detecting mini events were kept consistent across neurons, and data were quantified blind to genotype.

To evoke synaptic transmission by activating channelrhodopsin-2 (ChR2), we used a single-wavelength LED system (λ = 470 nm; CoolLED) connected to the epifluorescence port of the Olympus BX51 microscope. To restrict the size of the light beam for focal stimulation, a built-in shutter along the light path in the BX51 microscope was used. Light pulses of 0.5–1 ms triggered by a transistor-transistor logic (TTL) signal from the Clampex software (Molecular Devices) were used to evoke synaptic transmission. The light intensity at the sample was ~0.8 mW/mm^2. Electrophysiological data were acquired and analyzed using pCLAMP 10 software (Molecular Devices). IPSCs were recorded at 0 mV holding potential in the presence of 5 μM CNQX and 100 μM AP-5. Light pulses were delivered once every 10 s, and a minimum of 30 trials were collected. In paired-pulse recordings, 2 light pulses separated by 50, 100, or 150 ms were delivered. In cases that the first IPSC did not fully decay to baseline before the onset of the second IPSC, the baseline of the second IPSC was corrected before the peak was measured. To measure the kinetics of the IPSCs, averaged sweeps collected at the 150-ms interval were normalized, and the decay time constant and half-width were measured using automated procedures in the AxoGraph X 1.5.4 software.

To determine IPSC reversal potential (E_{IPSC}), IPSCs were recorded at varying holding potentials (20-mV steps) in the presence of CNQX (5 μM) and AP-5 (100 μM) to block AMPA receptors and NMDA receptors, respectively. IPSC amplitude was measured, and a linear regression was used to calculate the best-fit line, and the x-intercept was used as the E_{IPSC}. Under our recording conditions, the E_{IPSC} was ~–60 mV. Therefore, in the excitation/inhibition ratio (E/I) experiments, we recorded EPSCs at –60 mV and IPSCs at 0 mV holding potential. The only drug used for the E/I experiments was AP-5 (100 μM). In these experiments we used the same light intensity for evoking both IPSCs and EPSCs. In addition, we used similar stimulation regime for WT and *Disc1* LI mice, such that the peak amplitudes of IPSCs were comparable between genotypes.

For the experiments in which we optogenetically stimulated the MD axons in the mPFC, mice were excluded if the extent of infection in the MD was too large and leaked into surrounding brain regions. Rodent MD lacks INs; therefore all ChR2-infected neurons are expected to be relay projection neurons (Kuroda et al., 1998).

The latency and 10–90% rise time of EPSCs and IPSCs were calculated from either the averaged trace or individual sweeps for each cell using automated procedures in the AxoGraph X 1.5.4 software. ESPC and IPSC onset latency was calculated as the time from stimulation onset to 10% rise time, with EPSC-IPSC lag calculated as the difference. The 10% rise time has been reported to be a more reliable measure of delay to onset, as it minimizes the contribution of EPSC and IPSC rise time differences that are reflected in the time to peak (Mittmann et al., 2005). Some of the control data from WT mice used for comparing with *Disc1* LI mice (appearing in Figs. 3, 4) were previously reported in Delevich et al., 2015, (Figs. 1, 2, and 4).

Data analysis and statistics

All statistical tests were performed using Origin 9.0 (Origin-Lab) or GraphPad Prism 6.0 (GraphPad Software) software. All data were tested for normality using the D'Agostino–Pearson omnibus normality test to guide the selection of parametric or non-parametric statistical tests. Data are presented as mean ± SEM or median ± interquartile range as indicated. For parametric data, a two-tailed *t* test or two-way ANOVA was used, with a *post hoc* Sidak's test for multiple comparisons. For non-parametric data, a two-tailed Mann–Whitney *U* test was used; $p < 0.05$ was considered significant. A summary of the statistical analyses performed can be found in Table 1.

Results

Inhibitory synaptic transmission is reduced in adult *Disc1* LI mice

As a first estimation of inhibitory drive in the mPFC, we recorded mIPSCs onto L2/3 PNs in the dorsal anterior

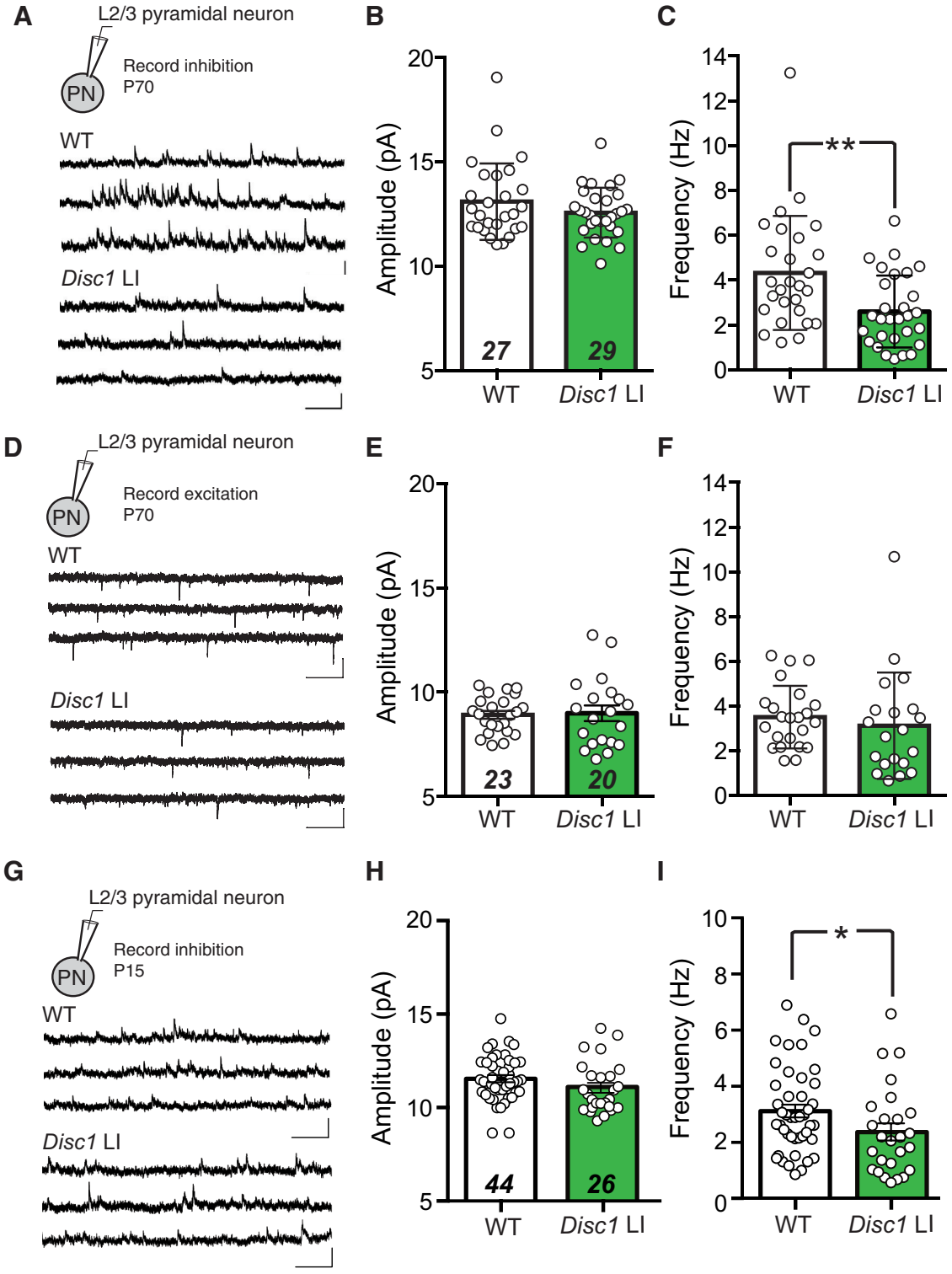

Figure 1. Reduced inhibitory synaptic transmission onto L2/3 pyramidal neurons in the mPFC of adult and juvenile *Disc1* LI mice. ***A***, Recording configuration and sample mIPSC traces recorded from L2/3 PNs in the mPFC of WT (upper) and *Disc1* LI (lower) mice at ~P70. ***B***, mIPSC amplitude (WT, $n = 27$ cells; *Disc1* LI, $n = 29$ cells). ***C***, mIPSC frequency (WT, $n = 27$ cells; *Disc1* LI, $n = 29$ cells; $^{**}p < 0.01$, Mann–Whitney *U* test). ***D***, Recording configuration and sample mEPSC traces recorded from L2/3 PNs in the mPFC of WT (upper) and *Disc1* LI (lower) mice at ~P70. ***E***, mEPSC amplitude (WT, $n = 23$ cells; *Disc1* LI, $n = 20$ cells). ***F***, mEPSC frequency (WT, $n = 23$ cells; *Disc1* LI, $n = 20$ cells). ***G***, Recording configuration and sample mIPSC traces recorded from L2/3 PNs in the mPFC

continued

of WT (upper) and *Disc1* LI (lower) mice at ~P15. mIPSC (***H***) amplitude (WT, $n = 44$ cells; *Disc1* LI, $n = 26$ cells; $p = 0.12$, *t* test) and (***I***) frequency (WT, $n = 44$ cells; *Disc1* LI, $n = 26$ cells; $*p < 0.05$, Mann–Whitney *U* test). All scale bars represent 20 pA, 500 ms. Bar graphs indicate median ± interquartile range (***B***, ***C***, ***F***, ***I***) or mean ± SEM (***E***, ***H***), as appropriate.

cingulate cortex (dACC) subregion of the mPFC in adult mice (P70). We found that compared with wild-type (WT) littermates, *Disc1* LI mice had significantly reduced mIPSC frequency (WT, 3.75 ± 3.25 Hz, $n = 27$ cells, $N = 6$; *Disc1* LI, 2.27 ± 2.72 Hz, $n = 29$ cells, $N = 5$; $U = 217.0$, $^{a}p < 0.01$, Mann–Whitney *U* test), but not amplitude (WT, 12.5 ± 2.48 pA, $n = 29$ cells, $N = 6$; *Disc1* LI, 12.52 ± 1.51 pA, $n = 27$ cells, $N = 5$; $U = 351.0$, $^{b}p = 0.51$, Mann–Whitney *U* test; Fig. 1*A–C*). The two groups did not differ in measures of mEPSCs (frequency: WT, 3.47 ± 1.97 Hz, $n = 23$ cells, $N = 4$; *Disc1* LI, 2.79 ± 2.4 Hz, $n = 20$ cells, $N = 5$; $U = 173.0$, $^{c}p = 0.17$, Mann–Whitney *U* test; amplitude: WT, 8.91 ± 0.18 pA; *Disc1* LI, 8.99 ± 0.37 pA, $t_{(41)} = 0.18$, $^{d}p = 0.86$, *t* test; Fig. 1*D–F*). Notably, we found that the frequency (but not amplitude) of mIPSCs recorded from dACC L2/3 PNs in *Disc1* LI mice was lower compared to their WT littermates at preweanling (~P15) age (amplitude: WT, $n = 44$ cells; *Disc1* LI, $n = 26$ cells; $^{e}p = 0.12$, *t* test; frequency: WT, $n = 44$ cells; *Disc1* LI, $n = 26$ cells; $^{f}p < 0.05$, Mann–Whitney *U* test; Fig. 1*G–I*). These data indicate that the inhibitory synaptic transmission is selectively impaired in the mPFC of *Disc1* LI mice, and that this impairment manifests early in postnatal development.

Altered presynaptic function of PV INs in *Disc1* LI mice

A reduction in mIPSC frequency could result from a decrease in synaptic transmission from one or more inhibitory IN populations. To investigate the source of reduced inhibitory drive onto L2/3 PNs in the mPFC of *Disc1* LI mice, we sought to examine the IPSCs originating from either PV or somatostatin (SOM) INs. To this end, we selectively expressed ChR2, the light-gated cation channel (Zhang et al., 2006), in PV or SOM INs by injecting the mPFC of *Disc1* LI*; PV-Cre* or *Disc1* LI*; SOM-Cre* mice, as well as their WT littermates, with an AAV expressing ChR2 in a Cre-dependent manner (AAV-DIO-ChR2 (H134R)-YFP). After viral expression had reached sufficient levels, we prepared acute brain slices and recorded light-evoked IPSCs onto L2/3 PNs in mPFC (Fig. 2*A*,*D*). We delivered paired light pulses (pulse duration 1 ms) with an interpulse interval of 50, 100, or 150 ms, and measured the ratio of the peak amplitude of the second IPSC over that of the first ($IPSC_2/IPSC_1$), also known as paired-pulse ratio (PPR; Fig. 2*B*,*E*). A similar technique was previously used to interrogate presynaptic GABA release from PV INs (Chu et al., 2012).

We found that the PPR of GABAergic transmission between PV INs and L2/3 PNs was significantly increased in the *Disc1* LI mice compared to their WT littermates at the 50- and 100-ms interpulse intervals (WT, $n = 13$ cells; *Disc1* LI, $n = 10$ cells; interval: $F_{(2,42)} = 6.77$, $^{g}p < 0.01$; genotype: $F_{(1,21)} = 10.77$, $p < 0.01$; interaction: $F_{(2,42)} = 3.92$, $p < 0.05$; two-way repeated-measures (RM) ANOVA followed by Sidak's tests; Fig. 2*C*), suggesting that GABA release from PV INs is impaired. In contrast, the PPR of GABAergic synaptic transmission from SOM INs to L2/3 PNs did not differ between genotypes (WT, $n = 15$ cells, *Disc1* LI, $n = 12$ cells; interval: $F_{(2,50)} = 24.88$, $^{h}p < 0.0001$; genotype: $F_{(1,25)} = 1.64$, $p = 0.21$; interaction $F_{(2,50)} = 0.47$, $p = 0.63$, two-way RM ANOVA; Fig. 2*F*). SOM-evoked IPSCs displayed significantly slower decay kinetics than PV-evoked IPSCs (Fig. 2*G*,*H*), consistent with previous reports (Koyanagi et al., 2010; Ma et al., 2012). No differences in IPSC kinetics were observed between *Disc1* LI mice and their WT littermates (cell type: $F_{(1,46)} = 90.82$, $^{i}p < 0.0001$; genotype: $F_{(1,46)} = 0.678$, $p = 0.41$; two-way ANOVA; Fig. 2*G*,*H*). In light of the observed reduction in mIPSC frequency, the increased PPR of PV-mediated IPSCs suggests that there is a presynaptic deficit in GABA release from PV cells to L2/3 PNs in the mPFC of *Disc1* LI mice.

Reduced feedforward inhibition (FFI) in a thalamus–mPFC circuit in *Disc1* LI mice

The mediodorsal nucleus of the thalamus (MD) sends major projections to the mPFC. This MD–mPFC circuit has been implicated in cognitive processes such as WM (Parnaudeau et al., 2013, 2018; Bolkan et al., 2017; Ferguson and Gao, 2018b) and cognitive flexibility (Parnaudeau et al., 2015; Rikhye et al., 2018) that are impaired in schizophrenia (Lesh et al., 2011; Parnaudeau et al., 2013, 2015). We and others have shown that excitatory inputs from the MD drive mPFC FFI (Miller et al., 2017; Collins et al., 2018; Meda et al., 2019) that is primarily mediated by mPFC PV INs (Delevich et al., 2015). Given the deficit in GABA release from PV INs to PNs in the mPFC of *Disc1* LI mice (Fig. 2), we reasoned that FFI in the MD–mPFC circuit may be affected in these mice. To test this hypothesis, we injected the MD of *Disc1* LI mice and their WT littermates with AAV-ChR2(H134R)-YFP. After viral expression reached sufficient levels, we used these mice to prepare acute brain slices, in which we recorded both excitatory and inhibitory synaptic transmission onto dACC L3 PNs in response to optogenetic stimulation of MD axons (Fig. 3*A*,*B*).

Brief (0.5 ms) light stimulation evoked monosynaptic EPSCs and disynaptic IPSCs onto L3 PNs in the dorsal mPFC (Fig. 3*C*; and see Delevich et al., 2015). We found that the contribution of inhibitory synaptic transmission to total synaptic inputs, measured as $IPSC^{peak}/(IPSC^{peak}+EPSC^{peak})$, or $I^{peak}/(I^{peak}+E^{peak})$, was significantly lower in *Disc1* LI mice than in WT mice when comparing the means of the two groups of animals (*Disc1* LI, 0.52 ± 0.03, $N = 11$ mice; WT, 0.70 ± 0.02, $N = 14$ mice; $t_{(23)} = 5.73$, $^{j}p < 0.0001$, *t* test; Fig. 3*D*), or the means of the two groups of neurons (*Disc1* LI, 0.60 ± 0.03; $n = 30$ cells, WT, 0.70 ± 0.02, $n = 40$ cells; $t_{(68)} = 3.17$, $^{k}p < 0.01$,

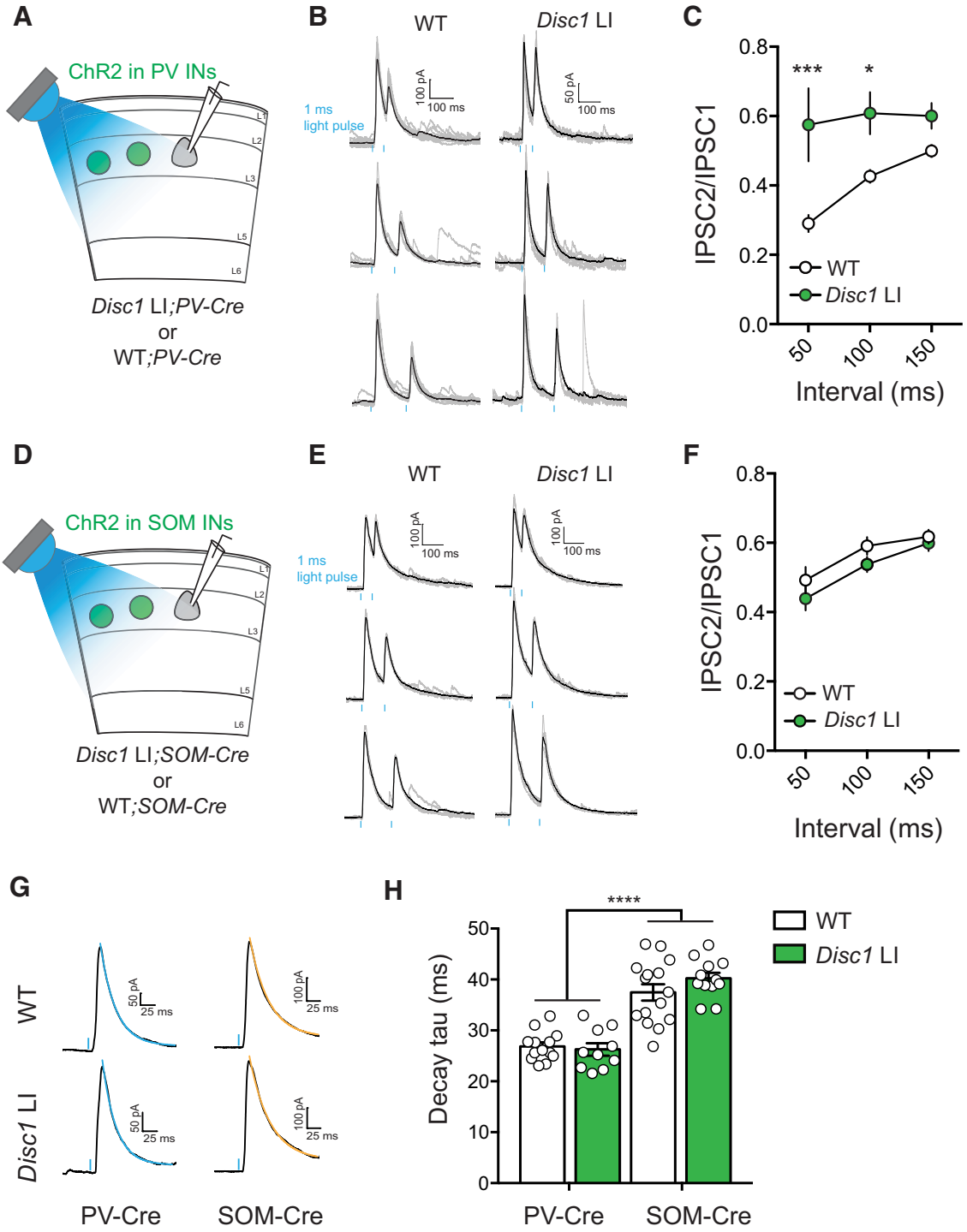

Figure 2. Altered presynaptic function of PV but not SOM INs in the mPFC of *Disc1* LI mice. ***A***, Schematic of the experimental configuration. ***B***, Sample traces of PV IN-mediated IPSCs recorded from WT (left panel) or *Disc1* LI (right panel) mice. Paired light pulses (1-ms duration; blue bars) were delivered at an interval of 50 ms (top), 100 ms (middle), or 150 ms (bottom). ***C***, Quantification of PPR for each genotype (WT, $n = 13$ cells; *Disc1* LI, $n = 10$ cells); $*p < 0.05$, $***p < 0.001$, two-way RM ANOVA followed by Sidak's test. ***D***, Schematic of the experimental configuration. ***E***, Sample traces of SOM IN-mediated IPSCs recorded from WT (left panel) or *Disc1* LI (right panel) mice. Paired light pulses (1-ms duration; blue bars) were delivered at an interval of 50 ms (top), 100 ms (middle), or 150 ms (bottom). ***F***, Quantification of PPR for each genotype (WT, $n = 15$ cells, *Disc1* LI, $n = 12$ cells). ***G***, Sample IPSC traces evoked by optogenetic stimulation of PV or SOM INs. Colored lines indicate exponential fits to the decays of the IPSCs. ***H***, Quantification of IPSC decay tau; $****p < 0.0001$, *t* test. Data in ***C***, ***F***, ***H*** are presented as mean ± SEM.

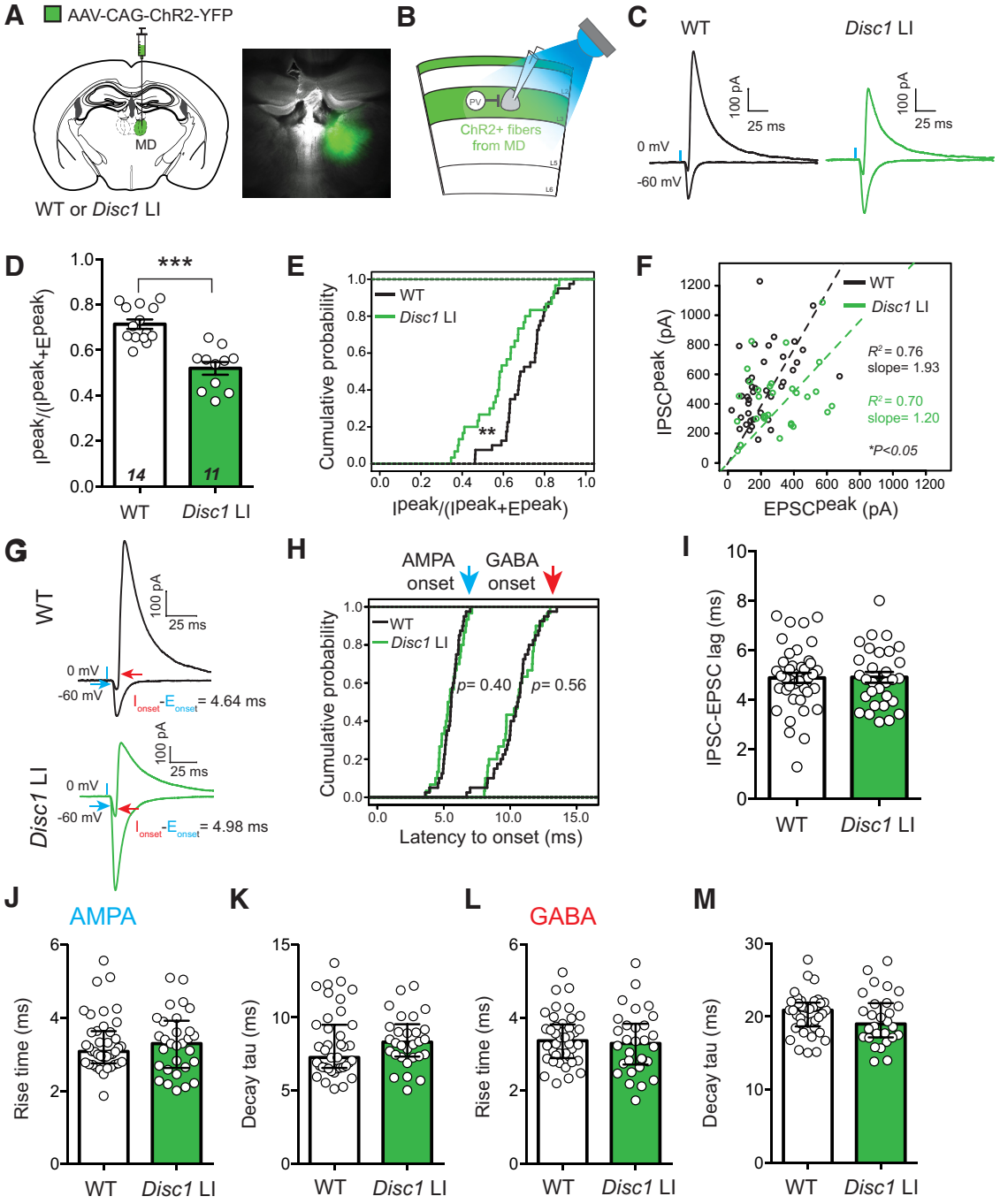

Figure 3. Reduced FFI in the MD–mPFC circuit in *Disc1* LI mice. ***A***, ***B***, Schematics of the experimental configuration. The right panel of ***A*** is an image of a brain section from a mouse used in electrophysiological recording, showing MD infected with AAV-CAG-ChR2-YFP. ***C***, Representative traces of evoked EPSC (recorded at –60 mV) and IPSC (recorded at 0 mV) from L3 PNs. ***D***, To estimate the relative recruitment of disynaptic FFI versus monosynaptic excitation, we divided peak IPSC (I^{peak}) by the sum of peak IPSC and peak EPSC ($I^{peak} + E^{peak}$). WT, $N = 14$ mice, *Disc1* LI, $N = 11$ mice; $***p < 0.001$, *t* test. ***E***, Same as in ***D***, except that the cumulative probability distributions of the values for individual neurons are shown. WT, $n = 40$ cells, *Disc1* LI, $n = 30$ cells; $**p < 0.01$, Kolmogorov–Smirnov test. ***F***, Scatter plot showing the peak amplitudes of IPSC and EPSC for individual neurons. Each circle represents one neuron (WT, $n = 30$ cells; *Disc1* LI, $n = 40$ cells). Dashed lines are linear regression lines for neurons in WT mice and *Disc1* LI mice. The slopes of the regression lines significantly differed at the 0.95 confidence level ($*p < 0.05$). ***G***, Sample traces of IPSC (recorded at 0 mV) and EPSC (recorded at –60 mV) recorded from L2/3 PNs in response to light-stimulation (blue bars) of MD axons. The latency to onset was measured from the time the light stimulus was triggered to the 10% EPSC (blue arrow) or IPSC (red arrow) rise time. Note that IPSC rise time was calculated from the peak of the inward current recorded at 0 mV. ***H***, Cumulative probability distributions for EPSC latency to onset (left) and IPSC latency to onset (right; EPSC, WT, $n = 40$ cells, *Disc1* LI, $n = 30$ cells, $p = 0.40$; IPSC, WT, $n = 40$ cells, *Disc1* LI, $n = 30$ cells, $p = 0.56$; Kolmogorov–Smirnov test). ***I***, Quantification of IPSC–EPSC lag,

continued

calculated as the difference in the latency to onset between the IPSC and the EPSC of each neuron (see also ***G***; WT, $n = 40$ cells, *Disc1* LI, $n = 30$ cells; $p > 0.05$, *t* test). ***J***, Quantification of the 10–90% EPSC rise time and decay tau (***K***; WT, $n = 40$ cells, *Disc1* LI, $n = 30$ cells; $p > 0.05$, Mann–Whitney *U* test). ***L***, Quantification of the 10–90% IPSC rise time and decay tau (***M***; WT, $n = 40$ cells, *Disc1* LI, $n = 28$ cells; $p > 0.05$, *t* test). Data are presented as median ± interquartile range (***J***, ***K***) or mean ± SEM (***D***, ***L***, ***M***).

t test; Fig. 3*E*). In addition, the slope of a linear regression describing the relationship between IPSC and EPSC peak amplitudes of individual neurons in the *Disc1* LI mice was significantly lower than that in WT (Fig. 3*F*). The latencies (Fig. 3*G–I*) and kinetics of the EPSCs (Fig. 3*J*,*K*) and IPSCs (Fig. 3*L*,*M*) in *Disc1* LI mice were similar to those in WT mice. These results together indicate that *Disc1* LI is associated with reduced MD-driven FFI in the mPFC.

Spontaneous excitatory synaptic transmission onto PV INs and their intrinsic properties are unchanged in *Disc1* LI mice

The decrease in FFI in the MD–mPFC pathway in *Disc1* LI mice could result from the impairment in GABA release from PV INs in the mPFC (Fig. 2), or reduced recruitment of mPFC PV INs by MD. Thalamically-driven FFI relies on the ability of PV INs to reach threshold in response to thalamic inputs, a process dependent on both synaptic and intrinsic properties of PV INs. DISC1 is expressed in MGE-derived inhibitory INs including PV INs (Schurov et al., 2004; Meyer and Morris, 2008; Steinecke et al., 2012; Seshadri et al., 2015) raising the possibility that *Disc1* LI could alter excitatory synaptic transmission onto PV INs and/or their intrinsic properties. We crossed the *Disc1* LI mouse line onto the *PV-Cre::tdTomato* lines, allowing us to assess the synaptic and intrinsic properties of visually identified PV INs in the context of *Disc1* LI. We found that mEPSC amplitude and frequency onto mPFC PV INs was consistent between genotypes (amplitude: WT, 12.39 ± 0.40 pA; *Disc1* LI, 13.48 ± 0.45 pA, $n = 20$, 23 cells/genotype, $N = 4$ mice/genotype; $t_{(41)} = 1.78$, $^{l}p = 0.08$; frequency: WT, 6.99 ± 0.74 Hz; *Disc1* LI, 6.55 ± 0.69 Hz, $t_{(41)} = 0.53$, $^{m}p = 0.60$; Fig. 4*A*,*B*). Next, we examined the intrinsic properties of PV INs in WT and *Disc1* LI mice and found no significant differences between genotypes (Fig. 4*C–H*), including minimum current injection required to elicit spiking (WT, 142.3 ± 12.67 pA; *Disc1* LI, 119.2 ± 14.3 pA, $t_{(24)} = 1.21$, $^{n}p = 0.24$; Fig. 4*G*) or maximum firing rate (WT, 88.92 ± 3.9 Hz; *Disc1* LI, 88.92 ± 6.78 Hz, $t_{(24)} = 0$, $^{o}P > 0.99$; Fig. 4*H*). These results suggest that neither intrinsic excitability of prefrontal PV INs nor spontaneous glutamatergic transmission onto them is grossly perturbed in *Disc1* LI mice.

Enhanced input but reduced output of PV INs in *Disc1* LI mice

We next examined recruitment of mPFC PV INs specifically within the MD–mPFC circuit to determine if reduced excitatory drive could account for the observed reduction in FFI in *Disc1* LI mice. We recorded evoked EPSCs onto PV IN and PN pairs in the mPFC in response to optogenetic stimulation of MD axons (Fig. 5*A*). We found that in WT mice, amplitudes of thalamocortical EPSCs were similar between PV INs and neighboring PNs (PV, −109.3 ± 109.7 pA, PN, −129.1 ± 103.2 pA, $n = 15$ pairs, $W = 0$, $^{p}p = 1.0$, Wilcoxon matched-pairs signed rank test; Fig. 5*B*,*C*). By contrast, in *Disc1* LI mice, thalamocortical EPSCs onto PV INs were much larger than those onto neighboring PNs (PV, −153.4 ± 211.9 pA; PN, −73.74 ± 104.6 pA; $n = 14$ pairs, W = −83, $^{q}p < 0.01$ Wilcoxon matched-pairs signed rank test; Fig. 5*B*,*C*). These data suggest that MD excitatory drive onto PV INs is enhanced relative to L2/3 PNs in the mPFC of *Disc1* LI mice. Therefore, reduced excitatory synaptic strength onto PV INs does not account for the decrease in FFI in the MD–mPFC circuit in *Disc1* LI mice compared with WT (Fig. 3).

Next, we probed presynaptic GABA release from PV cells within the MD–mFPC circuit, by optogenetically stimulating the MD axons (see the recording configuration in Fig. 3*A*,*B*) and measuring the PPR of MD-driven FFI onto mPFC PNs (Fig. 5*D*). Notably, we found that PPR of was significantly higher in *Disc1* LI mice than in WT mice (WT: 0.0 ± 0.1, $n = 24$ cells, $N = 10$; *Disc1* LI: 0.24 ± 0.34, $n = 17$ cells, $N = 6$; $U = 62$, $^{r}p = 0.0001$, two-tailed Mann–Whitney *U* test; Fig. 5*D*,*E*), mirroring the increase in PPR we observed when directly activating PV INs (Fig. 2*C*). In order to reduce variability in measuring the PPR, we set the light-stimulation such that there was no difference between genotypes in the average amplitude of the first evoked IPSCs (WT, 439.3 ± 41.31 pA, $n = 24$ cells, $N = 10$; *Disc1* LI, 367.1 ± 46.26 pA, $n = 17$ cells, $N = 6$; $t_{(39)} = 1.152$, $^{s}p = 0.256$, unpaired *t* test; Fig. 5*F*). Finally, we examined the relationship between PPR of MD-driven FFI and E-I ratio of MD-driven synaptic currents onto PNs. We found that there was a significant inverse correlation between FFI PPR and $I^{peak}/(I^{peak}+E^{peak})$ within PNs from *Disc1* LI mice but not WT mice (Fig. 5*G*). Together, our data suggest that in *Disc1* LI mice, GABA release from prefrontal PV INs is reduced, leading to decreased FFI in the MD–mPFC circuit.

Discussion

Perturbation of the multifunctional scaffolding protein DISC1 is linked to a range of behavioral phenotypes that are associated with major psychiatric disorders (Brandon and Sawa, 2011). These findings highlight DISC1 as a promising molecular lead to investigate the molecular pathways and neural circuits that underlie major mental illnesses (Niwa et al., 2016). Here, we used the *Disc1* LI mouse model to investigate the function of mPFC circuits that may be particularly relevant to the cognitive symptoms of psychiatric disorders. We found that *Disc1* LI mice exhibited elevated E-I ratio, measured as a reduction of spontaneous inhibitory transmission onto L2/3 PNs in mPFC and decreased FFI onto L2/3 PNs in the MD–mPFC circuit. Several lines of evidence suggest that this effect can be accounted for by a reduction in GABA

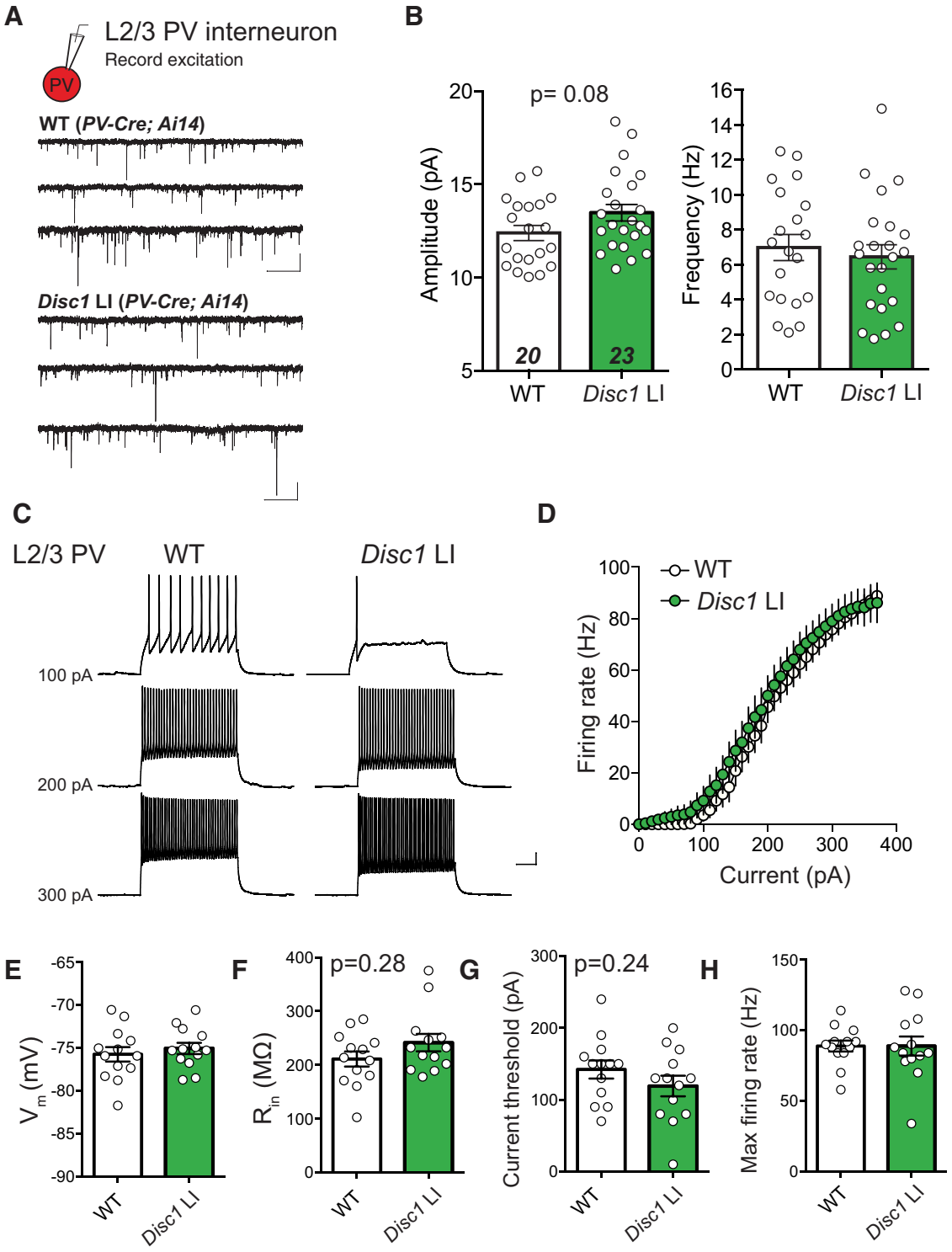

Figure 4. mEPSCs and intrinsic properties of PV INs are not altered in *Disc1* LI mice. ***A***, Recording configuration and sample mEPSC traces recorded from PV INs in WT (upper) and *Disc1* LI mice (lower). ***B***, Mean mEPSC amplitude (left) and median frequency (right; n = 20, 23 cells/genotype; N = 4 mice/genotype). ***C***, Sample traces from whole-cell current clamp recording of L2/3 PV IN in WT (left) and *Disc1* LI mouse in response to current injections. ***D***, Input-output curve showing average firing rate of PV INs in response to current injection in WT versus *Disc1* LI. ***E***, Resting membrane potential. ***F***, Input resistance. ***G***, Current threshold required to elicit spiking. ***H***, Maximum firing rate. Data in ***D***, ***E***, ***H*** shown as mean ± SEM. Data in ***F***, ***G*** shown as median ± interquartile range.

Table 1: Statistical tests and significance threshold used for each comparison

Data structure	Statistical test, *post hoc*	Significance threshold
[a]Non-normal distribution	Two-tailed Mann–Whitney *U* test	$p < 0.05$
[b]Non-normal distribution	Two-tailed Mann–Whitney *U* test	$p < 0.05$
[c]Non-normal distribution	Two-tailed Mann–Whitney *U* test	$p < 0.05$
[d]Normal distribution	Two-tailed unpaired *t* test	$p < 0.05$
[e]Normal distribution	Two-tailed unpaired *t* test	$p < 0.05$
[f]Non-normal distribution	Two-tailed Mann–Whitney *U* test	$p < 0.05$
[g]Normal distribution	Two-way RM ANOVA with *post hoc* Sidak's test	$p < 0.05$
[h]Normal distribution	Two-way RM ANOVA with *post hoc* Sidak's test	$p < 0.05$
[i]Normal distribution	Two-way ANOVA	$p < 0.05$
[j]Normal distribution	Two-tailed unpaired *t* test	$p < 0.05$
[k]Normal distribution	Two-tailed unpaired *t* test	$p < 0.05$
[l]Normal distribution	Two-tailed unpaired *t* test	$p < 0.05$
[m]Normal distribution	Two-tailed unpaired *t* test	$p < 0.05$
[n]Normal distribution	Two-tailed unpaired *t* test	$p < 0.05$
[o]Normal distribution	Two-tailed unpaired *t* test	$p < 0.05$
[p]Non-normal distribution	Wilcoxon matched-pairs signed ranks test	$p < 0.05$
[q]Non-normal distribution	Wilcoxon matched-pairs signed ranks test	$p < 0.05$
[r]Non-normal distribution	Two-tailed Mann–Whitney *U* test	$p < 0.05$
[s]Non-normal distribution	Two-tailed Mann–Whitney *U* test	$p < 0.05$

release from PV INs in the mPFC: 1) mIPSC frequency was significantly reduced onto L2/3 PNs in *Disc1* LI mice, consistent with a reduction in presynaptic release probability; 2) the PPR of IPSCs directly evoked by optogenetic stimulation of PV INs but not SOM INs was significantly increased in *Disc1* LI mice compared with WT; and 3) the PPR of MD-evoked FFI, which is almost exclusively driven by PV INs under the experimental conditions used (Delevich et al., 2015), was increased in *Disc1* LI mice and correlated with E-I ratio. Together, our findings suggest that PV → PN synapses are the primary site of impairment in the MD–mPFC circuit in *Disc1* LI mice.

It has been hypothesized that the cognitive deficits in psychiatric diseases may be the consequence of imbalanced excitation and inhibition (E-I) in key neural circuits (Kehrer et al., 2008; Lisman, 2012; Marin, 2012; Krystal et al., 2017; Ferguson and Gao, 2018a). Consistent with this hypothesis, several studies have shown that experimentally imposing elevated E-I within the mPFC impairs cognitive processing in rodents (Yizhar et al., 2011; Cho et al., 2015; Murray et al., 2015; Ferguson and Gao, 2018b). In addition to evidence of altered PV IN mediated inhibition, we observed that excitatory synaptic transmission onto PV cells driven by MD inputs was enhanced in *Disc1* LI mice, which could compensate for presynaptic deficits in PV IN function. Indeed, a recent study that examined multiple autism genetic mouse models found that increased E-I ratio did not drive network hyperexcitability but in fact led to homeostatic stabilization of excitability (Antoine et al., 2019). Therefore, potential network effects arising from altered E-I conductance ratios should not be over interpreted, and it remains unclear how the changes we observed in the *Disc1* LI mice affect network activity *in vivo* and resulting behavior.

In humans, *Disc1* polymorphisms are associated with measures of cognitive performance and frontal lobe structure among some ethnic groups (Burdick et al., 2005; Cannon et al., 2005; Hennah et al., 2005; Liu et al., 2006; Palo et al., 2007; Carless et al., 2011; Nicodemus et al., 2014). Multiple mouse models of DISC1 perturbation exhibit cognitive impairments (Koike et al., 2006; Clapcote et al., 2007; Li et al., 2007; Kvajo et al., 2008; Lipina et al., 2010; Niwa et al., 2010; Brandon and Sawa, 2011; Lee et al., 2013), strengthening the mechanistic link between DISC1 and cognition. Here we provide evidence of cell type-specific alterations within mPFC circuits implicated in multiples aspects of cognition. While we did not examine cognition in the *Disc1* LI mice, *Disc1* LI (−/−) mice are reported to exhibit blunted startle response and prepulse inhibition (PPI; Jaaro-Peled et al., 2018), a behavior that is regulated by the mPFC (Swerdlow et al., 2001; Schwabe and Koch, 2004). Future experiments interrogating mPFC-dependent cognition in *Disc1* LI mice will be critical for relating the circuit-level changes we observed in E-I balance and PV IN function to behavior.

While our study is the first to specifically detect a presynaptic deficit in PV INs in a DISC1 genetic deficiency model, previous studies using different transgenic models have reported that DISC1 influences inhibitory IN function or development: spontaneous IPSC frequency is reduced in the frontal cortex of male mice expressing truncated mouse DISC1 (Holley et al., 2013); PV IN function is impaired in the mPFC of mice overexpressing a truncated form of DISC1 (Sauer et al., 2015); PV expression is reduced in the PFC of several *Disc1* mouse models (Hikida et al., 2007; Shen et al., 2008; Niwa et al., 2010; Ayhan et al., 2011; Lee et al., 2013); and tangential migration of MGE-derived neurons is impaired by *Disc1* mutation or RNA interference (Steinecke et al., 2012; Lee et al., 2013). These findings provide converging evidence that DISC1 perturbation alters PFC inhibition. Our current findings more specifically implicate the presynapse of PV INs as a site of impairment in mice harboring a *Disc1* LI allele, which is the most extensively perturbed form of the gene reported to date (Shahani et al., 2015).

Several important caveats should be considered when interpreting our electrophysiology results. First, a reduction

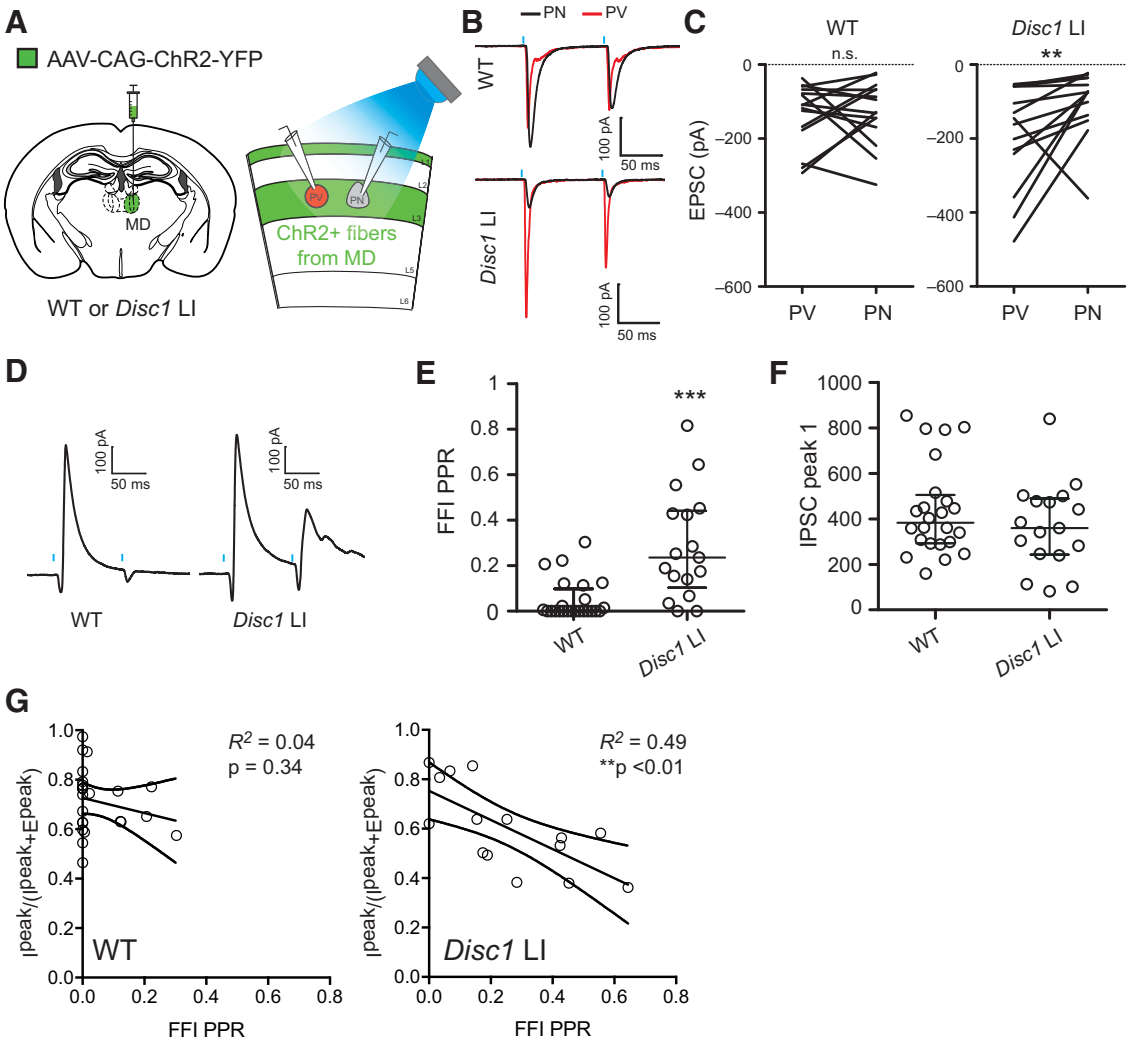

Figure 5. Altered presynaptic function of PV INs underlies the deficit of FFI in *Disc1* LI mice. ***A***, left, schematic of the experimental configuration. Right: schematic of the recording configuration in the mPFC acute slices. A Tdtomato$^+$ PV IN (red) and an adjacent PN (gray) in L3 of the mPFC were recorded simultaneously or sequentially. EPSCs onto these neurons were evoked by optogenetic stimulation (0.5-ms light pulses; blue bars) of MD axons. ***B***, Sample EPSC traces recorded from PV IN and PN pairs are superimposed and color-coded. ***C***, Quantification of the EPSC peak amplitude. n.s., not significant ($p = 1.0$); $**p < 0.01$; Wilcoxon matched-pairs signed ranks test. ***D***, Sample traces of FFI currents recorded from L3 PNs in response to optogenetic stimulation of MD axons. ***E***, Quantification of PPR of the MD-driven FFI onto L3 PNs; $***p < 0.001$, Mann–Whitney *U* test. ***F***, The mean amplitude of the first IPSC was consistent between genotypes. ***G***, FFI PPR plotted against $(I^{peak})/(I^{peak} + E^{peak})$; as seen in Fig. 3*D*) within cells shows that for *Disc1* LI mice but not WT mice, FFI PPR inversely correlated with $(I^{peak})/(I^{peak} + E^{peak})$, suggesting that synapses with high FFI PPR also exhibit higher E/I ratio; $**p < 0.01$. Data in ***E*** presented as median ± interquartile range data in ***F*** presented as mean ± SEM.

in mIPSC frequency is also consistent with a reduced number of inhibitory synapses. A recent study investigating *Disc1* LI mice reported no change in the number of PV INs themselves within the mPFC (Seshadri et al., 2015). In addition, we focused on PV and SOM IN function, which together comprise ~70% of cortical INs (Rudy et al., 2011). It is therefore possible that the remaining 30% of IN cell types, e.g., 5HT3a receptor-expressing neurons, also contribute to the reduced mIPSC frequency observed in *Disc1* LI mice. Next, IPSCs directly evoked by optogenetic stimulation significantly overlapped at short interstimulus intervals; therefore, changes in the input resistance due to open channels likely influenced the size of the second signal and hence the PPR measurement. More detailed analysis such as multiple probability-compound binomial analysis or direct analysis of failure rate is necessary to conclude that GABA release probability from PV INs is reduced in *Disc1* LI mice. We observed that PV IN evoked IPSC PPR was significantly increased at the 50- and 100-ms interstimulus intervals but not at the 150-ms interval. The time dependence of this effect may suggest a postsynaptic mechanism, such as GABA-mediated regulation of PPR (Kirischuk et al., 2002). Alternatively, $GABA_B$ presynaptic regulation may play a role in influencing PPR. Interestingly, a reduction in $GABA_B$ receptor expression in PNs has been observed in postmortem brain tissue of individuals with schizophrenia

(Mizukami et al., 2002). These caveats considered, we provide multiple lines of evidence that are consistent with elevated E-I balance and abnormal PV IN function in mPFC circuits in *Disc1* LI mice.

The coordinated activity between the MD and the PFC is important for WM, attention, and flexible goal-oriented behavior (Mitchell and Chakraborty, 2013; Parnaudeau et al., 2013, 2015; Schmitt et al., 2017; Alcaraz et al., 2018), faculties that are impaired in a variety of psychiatric disorders. Meanwhile, studies have found that MD–mPFC synaptic strength is modulated by social interaction, perhaps relevant to negative symptoms of schizophrenia and depression (Northoff and Sibille, 2014; Franklin et al., 2017; Zhou et al., 2017). In relation to DISC1, one study found that a common missense variant of *Disc1* was associated with altered thalamofrontal functional connectivity (Liu et al., 2015). Notably, patients with schizophrenia and bipolar disorder exhibit reduced MD-PFC functional connectivity relative to healthy controls (Welsh et al., 2010; Woodward et al., 2012; Anticevic et al., 2014). An emerging hypothesis posits that local disinhibition of PFC may destabilize the flow of information through the thalamofrontal loop and contribute to cognitive and negative symptoms in schizophrenia and related disorders (Anticevic et al., 2012; Murray and Anticevic, 2017). Structural alterations within thalamofrontal circuits have also been linked to cognitive deficits associated with aging (Hughes et al., 2012) and epilepsy (Pulsipher et al., 2009). However, until recently there was a paucity of data describing how the MD and frontal cortex interact at the neural circuit level. Recent studies have demonstrated that the MD thalamus recruits FFI in the rodent mPFC (Delevich et al., 2015; Miller et al., 2017; Collins et al., 2018; Meda et al., 2019) that is primarily mediated by PV INs (Delevich et al., 2015). Interestingly, chemogenetic excitation of mPFC PV INs has been shown to rescue cognitive deficits induced by chemogenetic inhibition of MD (Ferguson and Gao, 2018b).

Our findings extend data suggesting that MD, via its projections to PV INs, is a key regulator of E-I balance that underpins PFC circuit function. We demonstrate that reduced DISC1 expression, a key molecular candidate to study biology relevant to behavioral constructs related to several psychiatric disorders, leads to elevated E-I balance in the MD–mPFC thalamofrontal circuit. Given that few treatment options exist to address the cognitive symptoms of psychiatric disorders, efforts towards understanding the cellular and molecular mechanisms underlying abnormal thalamofrontal functional connectivity may yield therapies that will improve patient outcomes.

References

Alcaraz F, Fresno V, Marchand AR, Kremer EJ, Coutureau E, Wolff M (2018) Thalamocortical and corticothalamic pathways differentially contribute to goal-directed behaviors in the rat. Elife 7:e32517.

Anticevic A, Gancsos M, Murray JD, Repovs G, Driesen NR, Ennis DJ, Niciu MJ, Morgan PT, Surti TS, Bloch MH, Ramani R, Smith MA, Wang XJ, Krystal JH, Corlett PR (2012) NMDA receptor function in large-scale anticorrelated neural systems with implications for cognition and schizophrenia. Proc Natl Acad Sci USA 109:16720–16725.

Anticevic A, Cole MW, Repovs G, Murray JD, Brumbaugh MS, Winkler AM, Savic A, Krystal JH, Pearlson GD, Glahn DC (2014) Characterizing thalamo-cortical disturbances in schizophrenia and bipolar illness. Cereb Cortex 24:3116–3130.

Antoine MW, Langberg T, Schnepel P, Feldman DE (2019) Increased excitation-inhibition ratio stabilizes synapse and circuit excitability in four autism mouse models. Neuron 101:648–661.e4.

Ayhan Y, Abazyan B, Nomura J, Kim R, Ladenheim B, Krasnova IN, Sawa A, Margolis RL, Cadet JL, Mori S, Vogel MW, Ross CA, Pletnikov MV (2011) Differential effects of prenatal and postnatal expressions of mutant human DISC1 on neurobehavioral phenotypes in transgenic mice: Evidence for neurodevelopmental origin of major psychiatric disorders. Mol Psychiatry 16:293–306.

Beasley CL, Reynolds GP (1997) Parvalbumin-immunoreactive neurons are reduced in the prefrontal cortex of schizophrenics. Schizophr Res 24:349–355.

Bolkan SS, Stujenske JM, Parnaudeau S, Spellman TJ, Rauffenbart C, Abbas AI, Harris AZ, Gordon JA, Kellendonk C (2017) Thalamic projections sustain prefrontal activity during working memory maintenance. Nat Neurosci 20:987–996.

Brandon NJ, Sawa A (2011) Linking neurodevelopmental and synaptic theories of mental illness through DISC1. Nat Rev Neurosci 12:707–722.

Burdick KE, Hodgkinson CA, Szeszko PR, Lencz T, Ekholm JM, Kane JM, Goldman D, Malhotra AK (2005) DISC1 and neurocognitive function in schizophrenia. Neuroreport 16:1399–1402.

Cannon TD, Huttunen MO, Lonnqvist J, Tuulio-Henriksson A, Pirkola T, Glahn D, Finkelstein J, Hietanen M, Kaprio J, Koskenvuo M (2000) The inheritance of neuropsychological dysfunction in twins discordant for schizophrenia. Am J Hum Genet 67:369–382.

Cannon TD, Hennah W, van Erp TG, Thompson PM, Lonnqvist J, Huttunen M, Gasperoni T, Tuulio-Henriksson A, Pirkola T, Toga AW, Kaprio J, Mazziotta J, Peltonen L (2005) Association of DISC1/TRAX haplotypes with schizophrenia, reduced prefrontal gray matter, and impaired short- and long-term memory. Arch Gen Psychiatry 62:1205–1213.

Cardin JA, Carlén M, Meletis K, Knoblich U, Zhang F, Deisseroth K, Tsai LH, Moore CI (2009) Driving fast-spiking cells induces gamma rhythm and controls sensory responses. Nature 459:663–667.

Carless MA, Glahn DC, Johnson MP, Curran JE, Bozaoglu K, Dyer TD, Winkler AM, Cole SA, Almasy L, MacCluer JW, Duggirala R, Moses EK, Göring HH, Blangero J (2011) Impact of DISC1 variation on neuroanatomical and neurocognitive phenotypes. Mol Psychiatry 16:1096–1104, 1063.

Cho KK, Hoch R, Lee AT, Patel T, Rubenstein JL, Sohal VS (2015) Gamma rhythms link prefrontal interneuron dysfunction with cognitive inflexibility in Dlx5/6(+/−) mice. Neuron 85:1332–1343.

Chu HY, Ito W, Li J, Morozov A (2012) Target-specific suppression of GABA release from parvalbumin interneurons in the basolateral amygdala by dopamine. J Neurosci 32:14815–14820.

Clapcote SJ, Lipina TV, Millar JK, Mackie S, Christie S, Ogawa F, Lerch JP, Trimble K, Uchiyama M, Sakuraba Y, Kaneda H, Shiroishi T, Houslay MD, Henkelman RM, Sled JG, Gondo Y, Porteous DJ, Roder JC (2007) Behavioral phenotypes of Disc1 missense mutations in mice. Neuron 54:387–402.

Collins DP, Anastasiades PG, Marlin JJ, Carter AG (2018) Reciprocal circuits linking the prefrontal cortex with dorsal and ventral thalamic nuclei. Neuron 98:366–379.e4.

Delevich K, Tucciarone J, Huang ZJ, Li B (2015) The mediodorsal thalamus drives feedforward inhibition in the anterior cingulate cortex via parvalbumin interneurons. J Neurosci 35:5743–5753.

Ferguson BR, Gao WJ (2018a) PV interneurons: Critical regulators of E/I balance for prefrontal cortex-dependent behavior and psychiatric disorders. Front Neural Circuits 12:37.

Ferguson BR, Gao WJ (2018b) Thalamic control of cognition and social behavior via regulation of gamma-aminobutyric acidergic signaling and excitation/inhibition balance in the medial prefrontal cortex. Biol Psychiatry 83:657–669.

Franklin TB, Silva BA, Perova Z, Marrone L, Masferrer ME, Zhan Y, Kaplan A, Greetham L, Verrechia V, Halman A, Pagella S, Vyssotski AL, Illarionova A, Grinevich V, Branco T, Gross CT (2017) Prefrontal cortical control of a brainstem social behavior circuit. Nat Neurosci 20:260–270.

Fries P (2009) Neuronal gamma-band synchronization as a fundamental process in cortical computation. Annu Rev Neurosci 32:209–224.

Hashimoto T, Volk DW, Eggan SM, Mirnics K, Pierri JN, Sun Z, Sampson AR, Lewis DA (2003) Gene expression deficits in a subclass of GABA neurons in the prefrontal cortex of subjects with schizophrenia. J Neurosci 23:6315–6326.

Hayashi-Takagi A, Takaki M, Graziane N, Seshadri S, Murdoch H, Dunlop AJ, Makino Y, Seshadri AJ, Ishizuka K, Srivastava DP, Xie Z, Baraban JM, Houslay MD, Tomoda T, Brandon NJ, Kamiya A, Yan Z, Penzes P, Sawa A (2010) Disrupted-in-schizophrenia 1 (DISC1) regulates spines of the glutamate synapse via Rac1. Nat Neurosci 13:327–332.

Hennah W, Tuulio-Henriksson A, Paunio T, Ekelund J, Varilo T, Partonen T, Cannon TD, Lönnqvist J, Peltonen L (2005) A haplotype within the DISC1 gene is associated with visual memory functions in families with a high density of schizophrenia. Mol Psychiatry 10:1097–1103.

Hikida T, Jaaro-Peled H, Seshadri S, Oishi K, Hookway C, Kong S, Wu D, Xue R, Andradé M, Tankou S, Mori S, Gallagher M, Ishizuka K, Pletnikov M, Kida S, Sawa A (2007) Dominant-negative DISC1 transgenic mice display schizophrenia-associated phenotypes detected by measures translatable to humans. Proc Natl Acad Sci USA 104:14501–14506.

Hippenmeyer S, Vrieseling E, Sigrist M, Portmann T, Laengle C, Ladle DR, Arber S (2005) A developmental switch in the response of DRG neurons to ETS transcription factor signaling. PLoS Biol 3: e159.

Holley SM, Wang EA, Cepeda C, Jentsch JD, Ross CA, Pletnikov MV, Levine MS (2013) Frontal cortical synaptic communication is abnormal in Disc1 genetic mouse models of schizophrenia. Schizophr Res 146:264–272.

Hughes EJ, Bond J, Svrckova P, Makropoulos A, Ball G, Sharp DJ, Edwards AD, Hajnal JV, Counsell SJ (2012) Regional changes in thalamic shape and volume with increasing age. Neuroimage 63:1134–1142.

Ibi D, Nagai T, Koike H, Kitahara Y, Mizoguchi H, Niwa M, Jaaro-Peled H, Nitta A, Yoneda Y, Nabeshima T, Sawa A, Yamada K (2010) Combined effect of neonatal immune activation and mutant DISC1 on phenotypic changes in adulthood. Behav Brain Res 206:32–37.

Isaacson JS, Scanziani M (2011) How inhibition shapes cortical activity. Neuron 72:231–243.

Ishizuka K, Chen J, Taya S, Li W, Millar JK, Xu Y, Clapcote SJ, Hookway C, Morita M, Kamiya A, Tomoda T, Lipska BK, Roder JC, Pletnikov M, Porteous D, Silva AJ, Cannon TD, Kaibuchi K, Brandon NJ, Weinberger DR, Sawa A (2007) Evidence that many of the DISC1 isoforms in C57BL/6J mice are also expressed in 129S6/SvEv mice. Mol Psychiatry 12:897–899.

Ishizuka K, Kamiya A, Oh EC, Kanki H, Seshadri S, Robinson JF, Murdoch H, Dunlop AJ, Kubo K, Furukori K, Huang B, Zeledon M, Hayashi-Takagi A, Okano H, Nakajima K, Houslay MD, Katsanis N, Sawa A (2011) DISC1-dependent switch from progenitor proliferation to migration in the developing cortex. Nature 473:92–96.

Jaaro-Peled H, Kumar S, Hughes D, Kim S-H, Zoubovsky S, Hirota-Tsuyada Y, Zala D, Sumitomo A, Bruyere J, Katz BM, Huang B, Flores R, Narayan S, Hou Z, Economides AN, Hikida T, Wetsel WC, Deisseroth K, Mori S, Brandon NJ, et al. (2018) The corticostriatal circuit regulates sensorimotor gating via Disc1/Huntingtin-mediated Bdnf transport. bioRxiv 497446.

Kamiya A, Kubo K, Tomoda T, Takaki M, Youn R, Ozeki Y, Sawamura N, Park U, Kudo C, Okawa M, Ross CA, Hatten ME, Nakajima K, Sawa A (2005) A schizophrenia-associated mutation of DISC1 perturbs cerebral cortex development. Nat Cell Biol 7:1167–1178.

Kehrer C, Maziashvili N, Dugladze T, Gloveli T (2008) Altered excitatory-inhibitory balance in the NMDA-hypofunction model of schizophrenia. Front Mol Neurosci 1:6.

Kirischuk S, Clements JD, Grantyn R (2002) Presynaptic and postsynaptic mechanisms underlie paired pulse depression at single GABAergic boutons in rat collicular cultures. J Physiol 543:99–116.

Koike H, Arguello PA, Kvajo M, Karayiorgou M, Gogos JA (2006) Disc1 is mutated in the 129S6/SvEv strain and modulates working memory in mice. Proc Natl Acad Sci USA 103:3693–3697.

Koyanagi Y, Yamamoto K, Oi Y, Koshikawa N, Kobayashi M (2010) Presynaptic interneuron subtype- and age-dependent modulation of GABAergic synaptic transmission by beta-adrenoceptors in rat insular cortex. J Neurophysiol 103:2876–2888.

Krystal JH, Anticevic A, Yang GJ, Dragoi G, Driesen NR, Wang XJ, Murray JD (2017) Impaired tuning of neural ensembles and the pathophysiology of schizophrenia: A translational and computational neuroscience oerspective. Biol Psychiatry 81:874–885.

Kuroda M, Yokofujita J, Murakami K (1998) An ultrastructural study of the neural circuit between the prefrontal cortex and the mediodorsal nucleus of the thalamus. Prog Neurobiol 54:417–458.

Kvajo M, McKellar H, Arguello PA, Drew LJ, Moore H, MacDermott AB, Karayiorgou M, Gogos JA (2008) A mutation in mouse Disc1 that models a schizophrenia risk allele leads to specific alterations in neuronal architecture and cognition. Proc Natl Acad Sci USA 105:7076–7081.

Lee FH, Zai CC, Cordes SP, Roder JC, Wong AH (2013) Abnormal interneuron development in disrupted-in-schizophrenia-1 L100P mutant mice. Mol Brain 6:20.

Lesh TA, Niendam TA, Minzenberg MJ, Carter CS (2011) Cognitive control deficits in schizophrenia: Mechanisms and meaning. Neuropsychopharmacology 36:316–338.

Lewis DA, Curley AA, Glausier JR, Volk DW (2012) Cortical parvalbumin interneurons and cognitive dysfunction in schizophrenia. Trends Neurosci 35:57–67.

Li H, Penzo MA, Taniguchi H, Kopec CD, Huang ZJ, Li B (2013) Experience-dependent modification of a central amygdala fear circuit. Nat Neurosci 16:332–339.

Li W, Zhou Y, Jentsch JD, Brown RA, Tian X, Ehninger D, Hennah W, Peltonen L, Lönnqvist J, Huttunen MO, Kaprio J, Trachtenberg JT, Silva AJ, Cannon TD (2007) Specific developmental disruption of disrupted-in-schizophrenia-1 function results in schizophrenia-related phenotypes in mice. Proc Natl Acad Sci USA 104:18280–18285.

Lipina TV, Niwa M, Jaaro-Peled H, Fletcher PJ, Seeman P, Sawa A, Roder JC (2010) Enhanced dopamine function in DISC1-L100P mutant mice: implications for schizophrenia. Genes Brain Behav 9:777–789.

Lisman J (2012) Excitation, inhibition, local oscillations, or large-scale loops: what causes the symptoms of schizophrenia? Curr Opin Neurobiol 22:537–544.

Liu B, Fan L, Cui Y, Zhang X, Hou B, Li Y, Qin W, Wang D, Yu C, Jiang T (2015) DISC1 Ser704Cys impacts thalamic-prefrontal connectivity. Brain Struct Funct 220:91–100.

Liu YL, Fann CS, Liu CM, Chen WJ, Wu JY, Hung SI, Chen CH, Jou YS, Liu SK, Hwang TJ, Hsieh MH, Ouyang WC, Chan HY, Chen JJ, Yang WC, Lin CY, Lee SF, Hwu HG (2006) A single nucleotide polymorphism fine mapping study of chromosome 1q42.1 reveals the vulnerability genes for schizophrenia, GNPAT and DISC1: Association with impairment of sustained attention. Biol Psychiatry 60:554–562.

Ma Y, Hu H, Agmon A (2012) Short-term plasticity of unitary inhibitory-to-inhibitory synapses depends on the presynaptic interneuron subtype. J Neurosci 32:983–988.

Madisen L, Zwingman TA, Sunkin SM, Oh SW, Zariwala HA, Gu H, Ng LL, Palmiter RD, Hawrylycz MJ, Jones AR, Lein ES, Zeng H (2010) A robust and high-throughput Cre reporting and

characterization system for the whole mouse brain. Nat Neurosci 13:133–140.
Maher BJ, LoTurco JJ (2012) Disrupted-in-schizophrenia (DISC1) functions presynaptically at glutamatergic synapses. PLoS One 7: e34053.
Mao Y, Ge X, Frank CL, Madison JM, Koehler AN, Doud MK, Tassa C, Berry EM, Soda T, Singh KK, Biechele T, Petryshen TL, Moon RT, Haggarty SJ, Tsai LH (2009) Disrupted in schizophrenia 1 regulates neuronal progenitor proliferation via modulation of GSK3beta/beta-catenin signaling. Cell 136:1017–1031.
Marin O (2012) Interneuron dysfunction in psychiatric disorders. Nat Rev Neurosci 13:107–120.
Meda KS, Patel T, Braz JM, Malik R, Turner ML, Seifikar H, Basbaum AI, Sohal VS (2019) Microcircuit mechanisms through which mediodorsal thalamic input to anterior cingulate cortex exacerbates pain-related aversion. Neuron 102:944–959.e3.
Meyer KD, Morris JA (2008) Immunohistochemical analysis of Disc1 expression in the developing and adult hippocampus. Gene Expr Patterns 8:494–501.
Millar JK, Wilson-Annan JC, Anderson S, Christie S, Taylor MS, Semple CA, Devon RS, St Clair DM, Muir WJ, Blackwood DH, Porteous DJ (2000) Disruption of two novel genes by a translocation co-segregating with schizophrenia. Hum Mol Genet 9:1415–1423.
Miller OH, Bruns A, Ben Ammar I, Mueggler T, Hall BJ (2017) Synaptic regulation of a thalamocortical circuit controls depression-related behavior. Cell Rep 20:1867–1880.
Mitchell AS, Chakraborty S (2013) What does the mediodorsal thalamus do? Front Syst Neurosci 7:37.
Mittmann W, Koch U, Häusser M (2005) Feed-forward inhibition shapes the spike output of cerebellar Purkinje cells. J Physiol 563:369–378.
Mizukami K, Ishikawa M, Hidaka S, Iwakiri M, Sasaki M, Iritani S (2002) Immunohistochemical localization of GABAB receptor in the entorhinal cortex and inferior temporal cortex of schizophrenic brain. Prog Neuropsychopharmacol Biol Psychiatry 26:393–396.
Murray AJ, Woloszynowska-Fraser MU, Ansel-Bollepalli L, Cole KL, Foggetti A, Crouch B, Riedel G, Wulff P (2015) Parvalbumin-positive interneurons of the prefrontal cortex support working memory and cognitive flexibility. Sci Rep 5:16778.
Murray JD, Anticevic A (2017) Toward understanding thalamocortical dysfunction in schizophrenia through computational models of neural circuit dynamics. Schizophr Res 180:70–77.
Myles-Worsley M, Park S (2002) Spatial working memory deficits in schizophrenia patients and their first degree relatives from Palau, Micronesia. Am J Med Genet 114:609–615.
Nicodemus KK, Elvevåg B, Foltz PW, Rosenstein M, Diaz-Asper C, Weinberger DR (2014) Category fluency, latent semantic analysis and schizophrenia: A candidate gene approach. Cortex 55:182–191.
Niwa M, Kamiya A, Murai R, Kubo K-i, Gruber AJ, Tomita K, Lu L, Tomisato S, Jaaro-Peled H, Seshadri S, Hiyama H, Huang B, Kohda K, Noda Y, O'Donnell P, Nakajima K, Sawa A, Nabeshima T (2010) Knockdown of DISC1 by in utero gene transfer disturbs postnatal dopaminergic maturation in the frontal cortex and leads to adult behavioral deficits. Neuron 65:480–489.
Niwa M, Cash-Padgett T, Kubo KI, Saito A, Ishii K, Sumitomo A, Taniguchi Y, Ishizuka K, Jaaro-Peled H, Tomoda T, Nakajima K, Sawa A, Kamiya A (2016) DISC1 a key molecular lead in psychiatry and neurodevelopment: No-more disrupted-in-schizophrenia 1. Mol Psychiatry 21:1488–1489.
Northoff G, Sibille E (2014) Why are cortical GABA neurons relevant to internal focus in depression? A cross-level model linking cellular, biochemical and neural network findings. Mol Psychiatry 19:966–977.
Palo OM, Antila M, Silander K, Hennah W, Kilpinen H, Soronen P, Tuulio-Henriksson A, Kieseppä T, Partonen T, Lönnqvist J, Peltonen L, Paunio T (2007) Association of distinct allelic haplotypes of DISC1 with psychotic and bipolar spectrum disorders and with underlying cognitive impairments. Hum Mol Genet 16:2517–2528.
Parnaudeau S, O'Neill P-K, Bolkan SS, Ward RD, Abbas AI, Roth BL, Balsam PD, Gordon JA, Kellendonk C (2013) Inhibition of mediodorsal thalamus disrupts thalamofrontal connectivity and cognition. Neuron 77:1151–1162.
Parnaudeau S, Taylor K, Bolkan SS, Ward RD, Balsam PD, Kellendonk C (2015) Mediodorsal thalamus hypofunction impairs flexible goal-directed behavior. Biol Psychiatry 77:445–453.
Parnaudeau S, Bolkan SS, Kellendonk C (2018) The mediodorsal thalamus: an essential partner of the prefrontal cortex for cognition. Biol Psychiatry 83:648–656.
Pulsipher DT, Seidenberg M, Guidotti L, Tuchscherer VN, Morton J, Sheth RD, Hermann B (2009) Thalamofrontal circuitry and executive dysfunction in recent-onset juvenile myoclonic epilepsy. Epilepsia 50:1210–1219.
Rikhye RV, Gilra A, Halassa MM (2018) Thalamic regulation of switching between cortical representations enables cognitive flexibility. Nat Neurosci 21:1753–1763.
Rudy B, Fishell G, Lee S, Hjerling-Leffler J (2011) Three groups of interneurons account for nearly 100% of neocortical GABAergic neurons. Dev Neurobiol 71:45–61.
Sauer JF, Strüber M, Bartos M (2015) Impaired fast-spiking interneuron function in a genetic mouse model of depression. Elife 4.
Schizophrenia Working Group of the Psychiatric Genomics C (2014) Biological insights from 108 schizophrenia-associated genetic loci. Nature 511:421–427.
Schmitt LI, Wimmer RD, Nakajima M, Happ M, Mofakham S, Halassa MM (2017) Thalamic amplification of cortical connectivity sustains attentional control. Nature 545:219–223.
Schurov IL, Handford EJ, Brandon NJ, Whiting PJ (2004) Expression of disrupted in schizophrenia 1 (DISC1) protein in the adult and developing mouse brain indicates its role in neurodevelopment. Mol Psychiatry 9:1100–1110.
Schwabe K, Koch M (2004) Role of the medial prefrontal cortex in N-methyl-D-aspartate receptor antagonist induced sensorimotor gating deficit in rats. Neurosci Lett 355:5–8.
Seshadri S, Faust T, Ishizuka K, Delevich K, Chung Y, Kim SH, Cowles M, Niwa M, Jaaro-Peled H, Tomoda T, Lai C, Anton ES, Li B, Sawa A (2015) Interneuronal DISC1 regulates NRG1-ErbB4 signalling and excitatory-inhibitory synapse formation in the mature cortex. Nat Commun 6:10118.
Shahani N, Seshadri S, Jaaro-Peled H, Ishizuka K, Hirota-Tsuyada Y, Wang Q, Koga M, Sedlak TW, Korth C, Brandon NJ, Kamiya A, Subramaniam S, Tomoda T, Sawa A (2015) DISC1 regulates trafficking and processing of APP and Aβ generation. Mol Psychiatry 20:874–879.
Shen S, Lang B, Nakamoto C, Zhang F, Pu J, Kuan SL, Chatzi C, He S, Mackie I, Brandon NJ, Marquis KL, Day M, Hurko O, McCaig CD, Riedel G, St Clair D (2008) Schizophrenia-related neural and behavioral phenotypes in transgenic mice expressing truncated Disc1. J Neurosci 28:10893–10904.
Snitz BE, Macdonald AW 3rd, Carter CS (2006) Cognitive deficits in unaffected first-degree relatives of schizophrenia patients: A meta-analytic review of putative endophenotypes. Schizophr Bull 32:179–194.
Sohal VS, Zhang F, Yizhar O, Deisseroth K (2009) Parvalbumin neurons and gamma rhythms enhance cortical circuit performance. Nature 459:698–702.
Steinecke A, Gampe C, Valkova C, Kaether C, Bolz J (2012) Disrupted-in-schizophrenia 1 (DISC1) is necessary for the correct migration of cortical interneurons. J Neurosci 32:738–745.
Swerdlow NR, Geyer MA, Braff DL (2001) Neural circuit regulation of prepulse inhibition of startle in the rat: Current knowledge and future challenges. Psychopharmacology (Berl) 156:194–215.
Taniguchi H, He M, Wu P, Kim S, Paik R, Sugino K, Kvitsiani D, Kvitsani D, Fu Y, Lu J, Lin Y, Miyoshi G, Shima Y, Fishell G, Nelson SB, Huang ZJ (2011) A resource of Cre driver lines for genetic

targeting of GABAergic neurons in cerebral cortex. Neuron 71:995–1013.
Wang Q, Charych EI, Pulito VL, Lee JB, Graziane NM, Crozier RA, Revilla-Sanchez R, Kelly MP, Dunlop AJ, Murdoch H, Taylor N, Xie Y, Pausch M, Hayashi-Takagi A, Ishizuka K, Seshadri S, Bates B, Kariya K, Sawa A, Weinberg RJ, Moss SJ, Houslay MD, Yan Z, Brandon NJ (2011) The psychiatric disease risk factors DISC1 and TNIK interact to regulate synapse composition and function. Mol Psychiatry 16:1006–1023.
Wei J, Graziane NM, Gu Z, Yan Z (2015) DISC1 protein regulates γ-aminobutyric acid, type A (GABAA) receptor trafficking and inhibitory synaptic transmission in cortical neurons. J Biol Chem 290:27680–27687.
Welsh RC, Chen AC, Taylor SF (2010) Low-frequency BOLD fluctuations demonstrate altered thalamocortical connectivity in schizophrenia. Schizophr Bull 36:713–722.
Woodward ND, Karbasforoushan H, Heckers S (2012) Thalamocortical dysconnectivity in schizophrenia. Am J Psychiatry 169:1092–1099.
Yizhar O, Fenno LE, Prigge M, Schneider F, Davidson TJ, O'Shea DJ, Sohal VS, Goshen I, Finkelstein J, Paz JT, Stehfest K, Fudim R, Ramakrishnan C, Huguenard JR, Hegemann P, Deisseroth K (2011) Neocortical excitation/inhibition balance in information processing and social dysfunction. Nature 477:171–178.
Zhang F, Wang LP, Boyden ES, Deisseroth K (2006) Channelrhodopsin-2 and optical control of excitable cells. Nat Methods 3:785–792.
Zhang F, Wang LP, Brauner M, Liewald JF, Kay K, Watzke N, Wood PG, Bamberg E, Nagel G, Gottschalk A, Deisseroth K (2007) Multimodal fast optical interrogation of neural circuitry. Nature 446:633–639.
Zhou T, Zhu H, Fan Z, Wang F, Chen Y, Liang H, Yang Z, Zhang L, Lin L, Zhan Y, Wang Z, Hu H (2017) History of winning remodels thalamo-PFC circuit to reinforce social dominance. Science 357:162–168.